Liquid Crystals
Publication details, including instructions for authors and subscription information:
http://www.informaworld.com/smpp/title~content=t713926090

Growth of a SmA* phase in the microconfinement of a polymer network

H. K. Chan[a]; I. Dierking[a]
[a] School of Physics and Astronomy, University of Manchester, Schuster Laboratory, Manchester M13 9PL, UK

To cite this Article Chan, H. K. and Dierking, I.(2008) 'Growth of a SmA* phase in the microconfinement of a polymer network', Liquid Crystals, 35: 4, 507 — 512
To link to this Article: DOI: 10.1080/02678290801972096
URL: http://dx.doi.org/10.1080/02678290801972096

Liquid Crystals,
Vol. 35, No. 4, April 2008, 507–512

Growth of a SmA* phase in the microconfinement of a polymer network

H. K. Chan and I. Dierking*

School of Physics and Astronomy, University of Manchester, Schuster Laboratory, Oxford Road, Manchester M13 9PL, UK

(Received 29 August 2007; final form 8 January 2008)

The growth of a chiral smectic A (SmA*) phase after a temperature quench was investigated experimentally in the confinement of a stabilising polymer network. In contrast to the random orientation of bâtonnet domains observed for non-stabilised smectic growth, all the growing polymer-stabilised SmA* bâtonnets are aligned in the same direction, as a result of the interactions between the polymer network and the liquid crystal (LC). Interestingly, for each growing bâtonnet with long axis R, the early-time growth law changes from $R \sim t^{1/2}$ to $R \sim t$ for increasing quench depth, as is also observed for non-stabilised bâtonnet growth. This indicates that the previously reported crossover of the growth exponent from $n=½$ to $n=1$ for increasing quench depth may be universal, independent of sample dimension and confinement conditions. The growth dynamics of the SmA* phase is independent of the presence of the polymer network, even though interactions between the LC and the polymer network lead to clear structural influences.

Keywords: chiral smectic A phase; polymer network; microconfinement; bâtonnet growth

1. Introduction

Liquid crystals (LCs) have in recent years been shown to exhibit a variety of growth patterns and dynamic growth behaviour. After a temperature quench from the isotropic phase, growth of the stable LC phase occurs within the supercooled isotropic phase once the nucleating germs exceed a critical radius, R_C (*1–3*). For different LC phases, various growth patterns can be observed. These include circular germs (*4–6*), anisotropic bâtonnets (*7, 8*) and fractal aggregates (*9–11*). For the Euclidean growth of circular germs and bâtonnets, the growth dynamics can be described by a growth law $R \sim t^n$, where n is the growth exponent and R is a characteristic linear size of the growing germ. R can be the radius/diameter of a circular germ, or the long or short axis of a bâtonnet. For both radial and bâtonnet growth, the growth exponent generally changes from $n=½$ to $n=1$ for increasing quench depth, $T_m - T_0$ (*4–8*), where T_m and T_0 are the phase transition temperature and the externally applied temperature, respectively.

In the past decade, interest in polymer-modified LCs has increased significantly, because of a range of possible applications for polymer-dispersed liquid crystals (PDLCs) (*12*), e.g. as privacy windows. At the opposite end of the phase diagram, at low polymer concentrations, these systems are called polymer-stabilised liquid crystals (PSLCs) (*13*), which, for example, promise application in the field of electronic paper. Nevertheless, both polymer-dispersed as well as polymer-stabilised systems also merit investigation for fundamental reasons, especially as microconfined materials. In this study, we investigated the growth dynamics of a LC within a polymer network. A percolating polymer network is formed via photopolymerisation of mesogenic monomers within a particular LC phase, in this case the chiral smectic A (SmA*) phase of a ferroelectric LC mixture, as schematically illustrated in Figure 1(a). The network forms a template of the LC orientational order during the polymerization process (*14, 15*), but its local geometry is basically fractal in nature (*16*), with spatially varying void sizes in the order of microns and network-strand dimensions in the sub-micron regime, as shown in Figure 1b. The network morphology largely depends on the conditions during the polymerisation process (*17–19*). Because of the complicated geometry of the confining polymer network, the growth behaviour of a polymer stabilised LC phase after a temperature quench could potentially be very different as compared to a non-stabilised system. A fractal environment could induce fractal growth structures of the LC via long range elastic interactions, or the growth dynamics could be altered. This paper reports on the growth dynamics of a SmA* phase within a confining polymer network and comments on the influence on phase behaviour.

2. Experimental

The LC material employed was ZLI-5014-100, a commercially available multicomponent mixture previously supplied by Merck, Darmstadt. Its phase sequence on slow cooling is I 70.4°C N* 68°C SmA*

---

*Corresponding author. Email: ingo.dierking@manchester.ac.uk

ISSN 0267-8292 print/ISSN 1366-5855 online

DOI: 10.1080/02678290801972096
http://www.informaworld.com

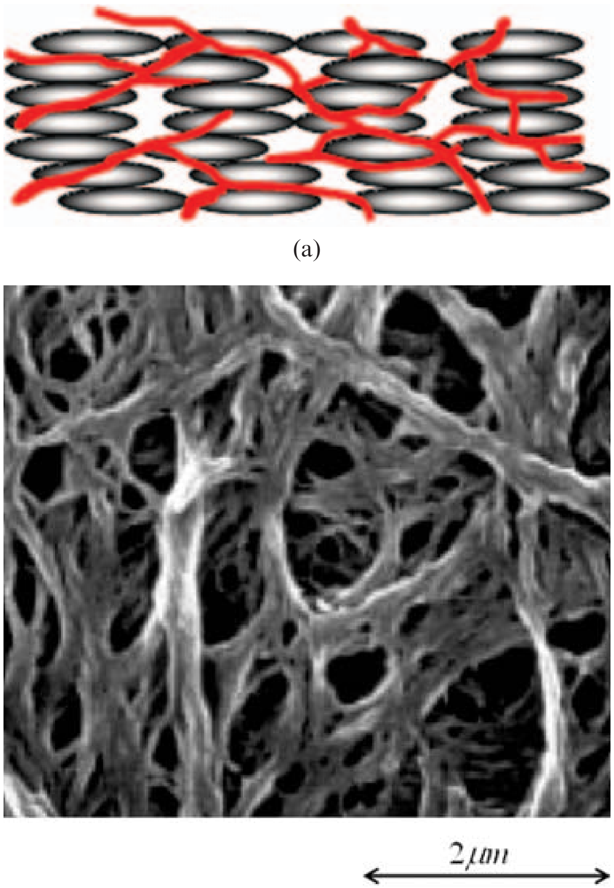

(a)

(b)

Figure 1. (a) Schematic illustration of a percolating polymer network formed within a SmA* phase (not drawn to scale). Polymer network and LC form a bi-continuous, phase-separated material. (b) Typical SEM morphology of a polymer network formed within a liquid crystalline phase. Micron-sized voids are filled with the LC whereas polymer network strands are generally on the sub-micron scale. Locally, the polymer network displays a fractal structure, whereas macroscopically it acts as a template for transferred orientational order of the LC.

64.5°C SmC* –11°C Cr. To produce the PSLC, the bifunctional monomer RM1, a diacrylate mesogen also from Merck, was added at a concentration of 7.5% by weight, together with a small amount of benzoin methyl ether (BME) to act as photoinitiator. Polymerisation was carried out in the SmA* phase at a peak wavelength of $\lambda=365\,\mathrm{nm}$ at a power density of $70\,\mathrm{mW\,cm^{-2}}$ for 5 min (Teklite UV source). Phase transition temperatures were slightly changed by the addition of the monomer/photoinitiator and during polymerisation, which is nevertheless not of direct relevance to the subsequent investigations, as we refer to quench depths, $T_m - T_0$.

The most prominent observation after the formation of the polymer network was that of the absence of a cholesteric phase, as compared to the neat LC mixture, the growth dynamics of which was investigated previously (*5*). This implies that the isotropic–cholesteric two-phase region is replaced by an isotropic–SmA* two-phase region. The polymer network that was formed in the non-helical SmA* phase obviously suppresses the helical structure of the cholesteric phase observed for the non-stabilised material. The elastic interactions in the microconfinement of an orientationally stabilising polymer network are stronger than the chiral interactions that promote helical superstructures. For the polymer-stabilised system we thus observe a direct transition from isotropic to SmA*.

Growth of the SmA* phase after a temperature quench from the isotropic phase was observed using a cell of $4\,\mu\mathrm{m}$ thickness, with polyimide alignment layers promoting planar molecular alignment of the SmA* phase. In the temperature-quench experiments, a Linkam TMS91 hot stage was employed for relative temperature control to 0.1 K. A quench rate of $3\,\mathrm{K\,min^{-1}}$ was applied for a best compromise between maximum achievable quench depths and electronic temperature regulation. The hot stage, which contains the Hele-Shaw cell, was placed on the rotation stage of a polarising optical microscope (Nikon Optiphot-Pol) for observation of LC growth. The growth process was captured by a digital camera (JVC KY-F1030U) at a time resolution of one image per second and at a spatial resolution of 1280×960 pixels, corresponding to an area of $520 \times 390\,\mu\mathrm{m}^2$. Growth data were obtained by measuring the long axis, R, of a growing bâtonnet as a function of time t, using the software ImageTool 3.0, developed at the University of Texas Health Science Center, San Antonio.

3. Results and discussion

An exemplary time series of smectic bâtonnet growth at a quench depth within the two-phase region is depicted in Figure 2(a) for the polymer-stabilised system. It can be seen that the anisotropic shape of the bâtonnets is equivalent to those of a non-stabilised isotropic to smectic material (Figure 2(b)). However, in contrast to the random orientation of the long bâtonnet axis of the latter, the polymer-stabilised samples exhibit a more or less uniform orientation of the bâtonnets along the orientational direction of the polymer network, which was formed in the SmA* phase. This emphasizes the fact that the polymer network acts like a macroscopic template of orientational order through elastic interactions with the LC. The local fractal structural features of the polymer network on the low micron size are not

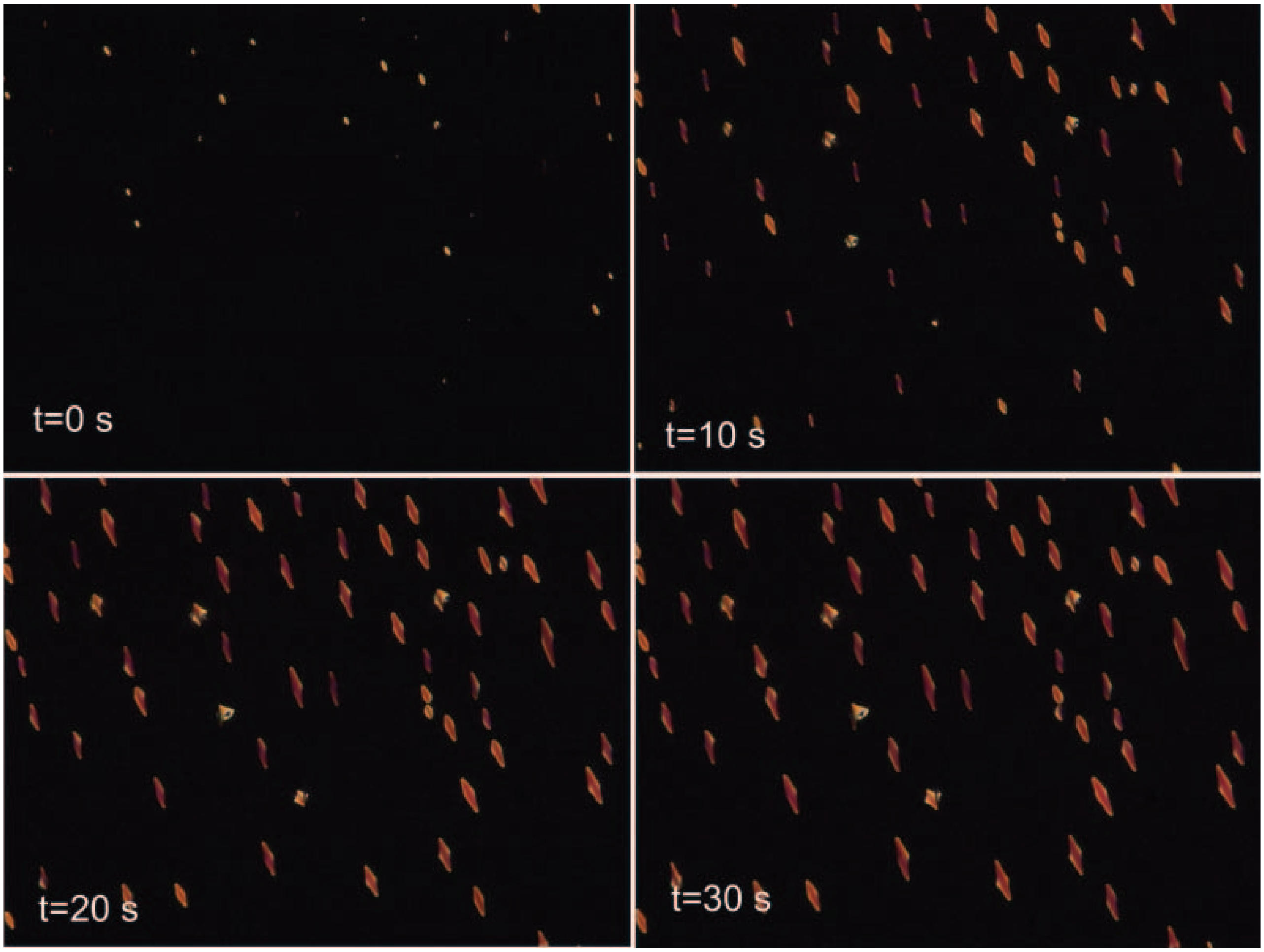

(a)

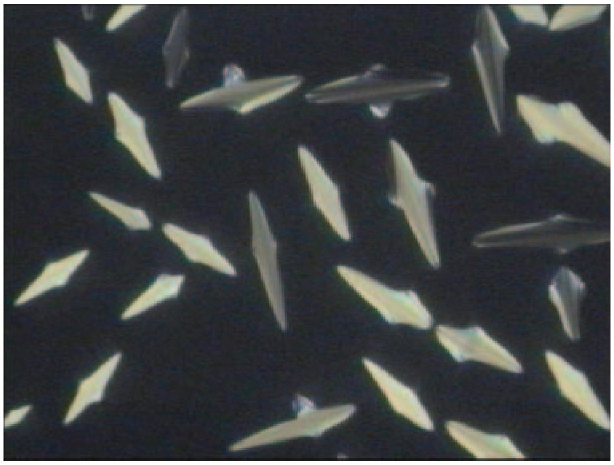

(b)

Figure 2. (a) Exemplary time series of bâtonnet growth of the polymer-stabilised SmA* phase (bright) of ZLI-5014-100 at a quench depth of $T_m - T_0 = 0.2\,K$ within the isotropic melt (dark). Note that the long axes of the bâtonnets are all uniformly oriented, implying network imposed orientational order of the director. The image size is 520 × $390\,\mu m^2$. (b) Comparative SmA* growth of a pure, non-stabilised material at the I–SmA* transition. The long axes of the smectic bâtonnets are practically isotropic in orientation (*20*) (I. Dierking, Textures of Liquid Crystals, p. 187 (2003). Copyright Wiley-VCH Verlag GmbH&Co. KGaA. Reproduced by permission).

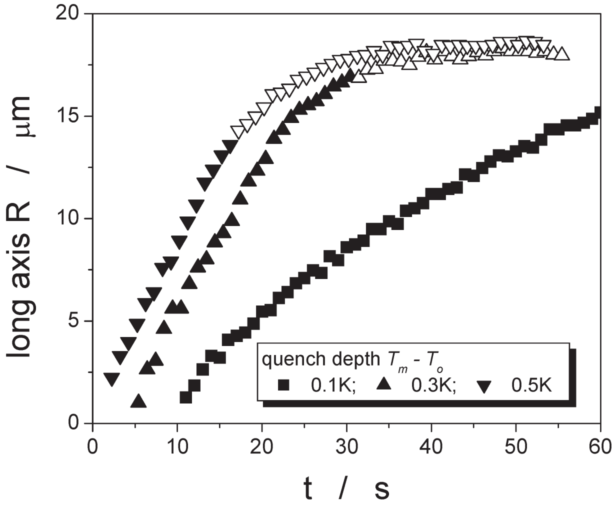

Figure 3. Exemplary growth data of the long SmA* bâtonnet axis as a function of time for several quench depths. Nucleus growth becomes faster for increasing supercooling, but also the growth dynamics changes from a square-root to a linear functionality. Full symbols indicate the data employed in further analysis, whereas open symbols represent regimes of saturation behaviour due to the nature of growth in two-phase regions.

sufficient in scale to also dominate at macroscopic dimensions of several tens of microns.

Figure 3 depicts the growth data of the long bâtonnet axis of the SmA* phase in the microconfinement of a stabilising polymer network as a function of time for several quench depths within the two-phase region of the LC mixture. Growth generally proceeds faster for larger quench depths and a saturation behaviour is observed at long times, because the quench is carried out into a two-phase region. The latter saturation regime is disregarded in the following investigations.

From the growth data, the growth exponent, *n*, can be determined as a function of quench depth, $T_m - T_0$, as shown in Figure 4. The characteristic growth exponent increases as the quench depth is increased and the data suggest a crossover from $n=½$ to $n=1$ as the quench depth changes from $T_m - T_0=0$ to $T_m - T_0>>0$. Such behaviour has also been observed for non-stabilised SmA* growth (*7*) and indeed also for the growth of cholesteric (*5, 6*), nematic (*4*) and blue phases (*21*). Figure 4 suggests that values of the growth exponent consistently seem to be slightly too large by approximately 0.1 (see dashed line in Figure 4). We attribute this to the uncertainty in available temperature control, which was 0.1 K. Unfortunately, further experiments at larger quench depths could not be carried out, because nucleation was observed before reaching quench depths larger than $T_m - T_0>0.5$ K, which implies that growth could not be followed at isothermal conditions at such supercooling. Taking into account various sources of error, especially limitations in temperature control, the growth dynamics of Figure 4 suggests a crossover of the growth exponent from $n=½$ to $n=1$ for a quench depth regime between $0\,\mathrm{K}<T_m - T_0<1\,\mathrm{K}$. This is consistent with investigations on materials that are not polymer-stabilised and suggests that microconfinement does not alter the growth laws significantly, whereas it does alter the mesomorphism and the macroscopic germ orientation.

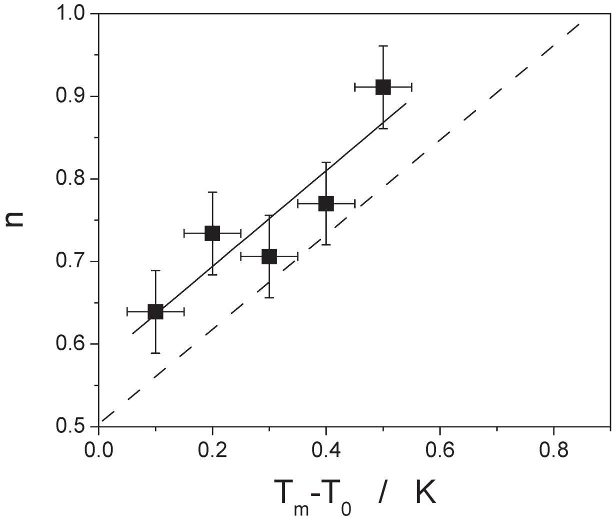

Figure 4. Experimental growth exponent, *n*, as a function of quench depth, $T_m - T_0$, (symbols) for the growth of the polymer-stabilised SmA* phase of ZLI-5014-100. The solid line represents a guide to the eye. It seems that the experimentally determined growth exponent, *n*, is consistently slightly too large by a constant factor of 0.1 (dashed line as a guide to the eye).

The observed crossover in dynamic growth scaling seems to be quite general, independent of liquid crystalline phase or confinement conditions, even independent of mesogenic behaviour at all. Nevertheless, a satisfying theoretical explanation has still to be found. We believe that a possible explanation lies in the thermal diffusion properties of the latent heat generated at the phase boundary during the isotropic to liquid crystalline phase transition (*22*).

Employing a multicomponent LC mixture implies that a two-phase region is observed at the isotropic–LC transition. This means that only a certain LC volume fraction is formed within the isotropic melt, depending on quench depth, which dictates the two-phase equilibrium. The LC volume fraction, ϕ_{LC}, increases with increasing quench depth, as illustrated in the texture series of Figure 5. From these images it is also clear that the number of germs increases drastically with increasing quench depth, whereas the

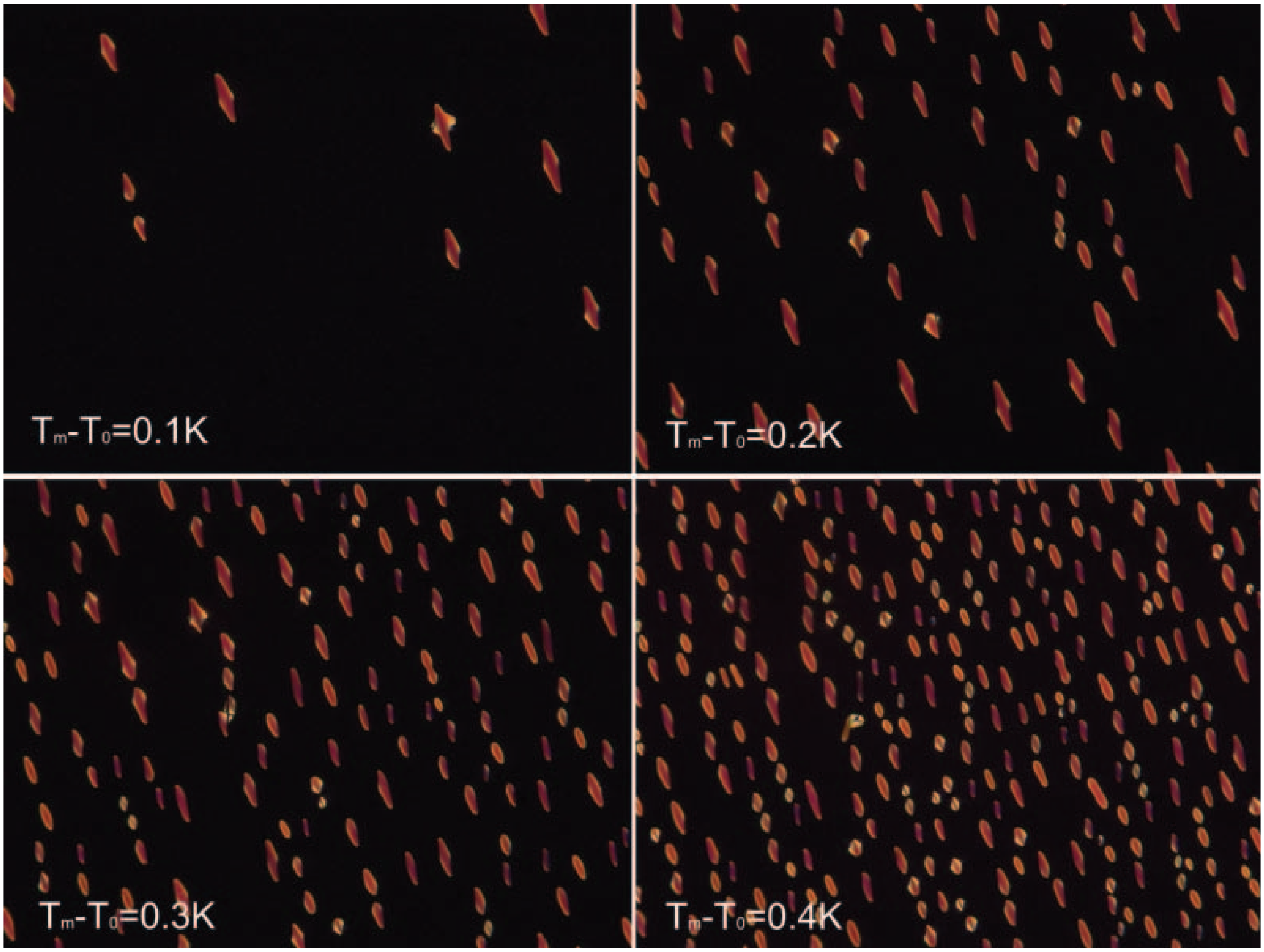

Figure 5. Equilibrium late-time images at various quench depths for the growth of the polymer-stabilised SmA* phase of ZLI-5014-100. For increasing quench depth the LC volume fraction obviously increases, but also more germs of a smaller size are observed. Again, macroscopic orientational order of the long smectic bâtonnet axis is clearly evident.

final germ size decreases. (At very long times, Ostwald ripening and coarsening processes may again decrease the number of germs and increase their size, but this time regime is not the subject of this investigation).

Corresponding volume fractions, ϕ_{LC}, as a function of reduced temperature, $T_{\mathrm{m}} - T_0$, obtained by quasi-static cooling, are shown in Figure 6. The LC volume fraction linearly increases with decreasing temperature to a point of approximately equal volume fractions of the LC and the isotropic phase, i.e. $\phi_{\mathrm{LC}} \approx 0.5$. Only for lower temperatures, does the relationship become nonlinear and displays saturation behaviour. We note that the temperature interval, in which the crossover of the growth exponent n occurs, only represents a small range within the linear volume fraction regime close to the phase transition temperature T_{m}, as indicated in Figure 6. At these low volume fractions of the LC phase, thus small quench depths $T_{\mathrm{m}} - T_0$, the LC volume fraction, ϕ_{LC}, obtained from quasi-static cooling is practically equivalent to that observed in the quench experiments, as demonstrated by the inset in Figure 6.

4. Conclusions

We have investigated the growth dynamics of smectic liquid crystalline germs within the microconfinement of a polymer network in terms of universal growth laws, $R \sim t^n$. The growth exponent n exhibits a crossover from $n=½$ to $n=1$ for increasing quench depth, as also observed for other, non-stabilised liquid crystalline materials. A confining polymer network thus does not alter the fundamental LC growth dynamics, even though mesomorphism, as well as germ orientation, is altered by the network. This implies that interactions between a LC and a dispersed polymer network are larger than chiral interactions forming a (long pitch) helical

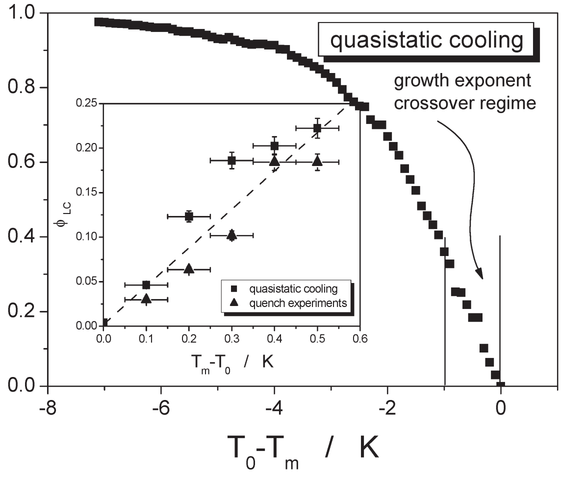

Figure 6. Equilibrium volume fraction, ϕ_{LC}, of the polymer-stabilised SmA* phase obtained by quasi-static cooling, as a function of reduced temperature, $T_m - T_0$. The inset shows comparable equilibrium fractions of the polymer-stabilised SmA* phase obtained by temperature quench (triangles) and quasi-static cooling (squares), implying that two-phase equilibrium of the mixture is the reason for the stoppage of growth at late times.

superstructure. The crossover regime of the growth exponent is located in a small temperature range within the two-phase region, close to the upper phase transition temperature of the isotropic–LC transition.

References

(1) Ratke L.; Voorhees P.W. *Growth and Coarsening*; Springer: Berlin, 2002.
(2) Bray A.J. *Adv. Phys.* **1994**, *43*, 357–459.
(3) Hohenberg P.C.; Halperin B.I. *Rev. Mod. Phys.* **1977**, *49*, 435–479.
(4) Diekmann K.; Schumacher M.; Stegemeyer H. *Liq. Cryst.* **1998**, *25*, 349–355.
(5) Dierking I. *J. Phys. Chem. B* **2000**, *104*, 10642–10646.
(6) Dierking I. *Appl. Phys. A* **2001**, *72*, 307–310.
(7) Dierking I.; Russell C. *Physica B* **2003**, *325*, 281–286.
(8) Chan H.K.; Dierking I. *Phys. Rev. E* **2004**, *70*, 021703.
(9) Baehr C.; Ebert M.; Frick G.; Wendorff J.H. *Liq. Cryst.* **1990**, *7*, 601–606.
(10) Dierking I. *ChemPhysChem* **2001,** *2,* 59–62; Dierking, I. *J. Phys. condensed Matter* **2001,** *13,* 1353–1360.
(11) Dierking I.; Chan H.K.; Culfaz F.; McQuire S. *Phys. Rev. E* **2004**, *70*, 051701.
(12) Kitzerow H.-S. *Liq. Cryst.* **1994,** *16,* 1–31; Bouteiller, L.; Le Barny, P. *Liq. Cryst.* **1996,** *21,* 157–174; Higgins, D.A. *Adv. Mater.* **2000,** *12,* 251–264.
(13) Dierking I. *Adv. Mater.* **2000**, *12*, 167–181.
(14) Fung Y.K.; Yang D.-K.; Ying S.; Chien L.-C.; Zumer S.; Doane J.W. *Liq. Cryst.* **1995,** *19,* 797–801; Fung, Y.K.; Borstnik, A.; Zumer, S.; Yang, D.-K.; Doane, J.W. *Phys. Rev. E* **1997,** *55,* 1637–1645.
(15) Dierking I.; Kosbar L.L.; Afzali-Ardakani A.; Lowe A.C.; Held G.A. *J. Appl. Phys.* **1997,** *81,* 3007–3014; Held, G.A.; Kosbar, L.L.; Dierking, I.; Lowe, A.C.; Grinstein, G.; Lee, V.; Miller, R.D. *Phys. Rev. Lett.* **1997,** *79,* 3443–3446.
(16) Dierking I. *J. Phys. D* **2002,** *35,* 2520–2525; Dierking, I. *Adv. Mater.* **2003,** *15,* 152–156; Dierking, I. *Adv. Funct. Mater.* **2004,** *14,* 883–890.
(17) Rajaram C.V.; Hudson S.D.; Chien L.-C. *Chem. Mater.* **1995,** *7,* 2300–2308; Rajaram, C.V.; Hudson, S.D.; Chien, L.-C. *Chem. Mater.* **1996,** *8,* 2451–2460; Rajaram, C.V.; Hudson, S.D.; Chien, L.-C. *Polymer* **1998,** *39,* 5315–5319.
(18) Fuh A.Y.-G.; Tsai M.-S.; Huang C.-Y. *Jap. J. Appl. Phys.* **1996**, *35*, 3960–3963.
(19) Dierking I.; Kosbar L.L.; Lowe A.C.; Held G.A. *Liq. Cryst.* **1998,** *24,* 387–395; Dierking, I.; Kosbar, L.L.; Lowe, A.C.; Held, G.A. *Liq. Cryst.* **1998,** *24,* 397–406.
(20) Dierking I. *Textures of Liquid Crystals*; Wiley-VCH: Weinheim, 2003.
(21) Demikov E.; Stegemeyer H.; Blümel T. *Phys. Rev. E* **1994**, *49*, R4787–R4790.
(22) Löwen H.; Bechhoefer J.; Tuckerman L.S. *Phys. Rev. A* **1992,** *45,* 2399–2415; Chan, H.K. Ph.D. Thesis, *Growth of Supercooled Liquid Crystals*; University of Manchester: UK, 2007; Chan, H.K.; Dierking, I. *Phys. Rev. E*, in press.